

Original

# The Induction and the Chronological Observation of Congenital Spinal Deformities in Mice with 7T Magnetic Resonance Microscopy

Haruki Ueda<sup>1)</sup>, Takuya Iimura<sup>1)</sup>, Hiroshi Moridaira<sup>1)</sup>, Satoshi Inami<sup>1)</sup>,  
Hiromichi Aoki<sup>1)</sup>, Yoshiteru Seo<sup>2)†</sup>, Hiroshi Taneichi<sup>1)</sup>

<sup>1)</sup> Department of Orthopaedic Surgery, Dokkyo Medical University 880 Kitakobayashi, Mibumachi, Shimotsuga, Tochigi, Japan zip 321-0293

<sup>2)</sup> Department of Regulatory Physiology, Dokkyo Medical University School of Medicine 880 Kitakobayashi, Mibumachi, Shimotsuga, Tochigi, Japan zip 321-0293

† Present address : Faculty of Home Economics, Aichi Gakusen University, Okazaki, 444-8520, Japan

## SUMMARY

**Purpose** : To set up high-resolution magnetic resonance imaging capable of observing chronologically on congenital scoliosis mouse models *in vivo* using 7 tesla (T) magnetic resonance imaging.

**Methods** : The mouse models of congenital scoliosis were created by maternal carbon monoxide exposure. The new-born mice were screened by soft X-ray, and those with spinal anomalies were followed alive with repetitive soft X-ray image and 7T MR images. Using a surface coil, three dimensional T<sub>1</sub>-weighted gradient-echo MR (3D-T<sub>1w</sub>) images and three dimensional T<sub>2</sub>-weighted rapid acquisition with relaxation enhancement MR (3D-T<sub>2w</sub>) images were obtained with a final resolution of 50 μm. MRI measurements were performed 3 times in each mouse until 3 months after birth. Then, the mice were euthanized and fixed by paraformaldehyde, and a set of MRI was measured.

**Results** : Three congenital vertebral anomalies in two mice were created. They were one block vertebra, one unsegmented hemivertebra, and one adjacent wedge vertebrae. All of them did not change morphologically from 1.5 to 3 months after birth. MR images clearly showed the morphology of the anomalies which had characteristics of the non-progressive congenital vertebral anomalies in human studies.

**Conclusion** : Morphological changes in the vertebral anomalies of mice could be detected and chronologically followed alive by soft X-ray and 7T MR imaging. While soft X-ray image could provide their global spinal alignment, MR imaging could depict the local morphology comparable to low-powered light microscopy distinguishing osseous and intervertebral structures of the small mice spine as well as small arteries around the spine.

**Key Words** : Congenital scoliosis mouse, vertebral anomalies, Magnetic Resonance Imaging, Chronological follow up

## INTRODUCTION

Congenital scoliosis is a spinal deformity caused by vertebrae that were not properly formed or segmentalized before birth. Its clinical course of the patients with these anomalies varies depending on the location,

Received March 29, 2021 ; accepted April 28, 2021

Reprint requests to : Haruki Ueda, MD.

Department of Orthopaedic Surgery, Dokkyo Medical University 880 Kitakobayashi, Mibumachi, Shimotsuga, Tochigi 321-0293, Japan

numbers, and shape of these vertebrae, ranging from asymptomatic to life threatening due to chronic respiratory insufficiency resulting from insufficient lung and thoracic cage development<sup>1,2</sup>). To prevent this devastating course, surgical interventions are required at earlier life stage before their deformities progress, which are basically to resect abnormal vertebrae, to correct the curve, and to fuse the spine as corrected. But spinal fusion surgery for the growing children is notorious for the higher incidence of the surgical complications and revision surgeries<sup>3~5</sup>). The incidence of complications in the congenital scoliosis surgeries are reported as especially high among other scoliosis categories, with 10% in total complications, 2% in neurological deficit, and 0.3% of the mortality rate<sup>5</sup>). Long spinal fusion surgeries for growing young children are also known to have risk for the restrictive lung disease and thoracic insufficiency syndrome<sup>3,4</sup>). Hence, it is critical for the treatment of the congenital scoliosis to predict which, when, and how much the spinal deformity progress, in order to perform proper surgery at the proper timing before the curve progresses significantly.

However, we are still lacking sufficient evidence which vertebral anomaly should be surgically corrected. In the current clinical settings, X-ray images and CT scan images are the standard modalities to assess these deformities. Whole spine X-ray images can provide the global appearance of the spinal malalignment. The CT scan provides very detailed morphological information especially of osseous structures within a minute of scanning time. In the chronological follow-up of global changes with X-ray images and local information with CT images, the prediction of the deformity progression is made within the context of the growth of the patients<sup>6,7</sup>). Osseous continuation and the existence of the intervertebral structures around the abnormal vertebrae depicted by the CT images are evaluated for additional information for the prediction. However, there are some downsides of the CT images. The CT images cannot present the soft tissue structures in detail such as intervertebral discs, cartilages, neural tissues, which are expected to be abnormally formed nearby the vertebral anomalies. Moreover, although easier access to these modalities, their radiation exposure, repetitively in many cases, to

the growing children has been concerning. On the contrary, Magnetic Resonance Imaging (MRI) can provide us with more elaborate observation including soft tissue structures without radiation exposure. It takes longer imaging time and often requires younger patients to be sedated, which set the hurdle higher for its use among them. Therefore, currently MRI are not widely considered as one of the routine tools to follow up the pediatric congenital spinal deformities. No such report could be found currently that attempted to find any features of the vertebral deformity which would progress based on the MRI findings.

Animal studies on congenital scoliosis have been reported<sup>8~11</sup>). Hypoxia plays a role in disrupting the embryonic vertebral development, and some authors succeeded in creating congenital scoliosis mice by CO exposure to the fetus<sup>9</sup>). Loder et al. reported the induction of congenital spinal deformities by exposing CO to maternal mice at certain point of the pregnancy<sup>11</sup>). Farley et al. used the similar method to create spinal deformity model mice and surveyed if those deformities progressed<sup>10</sup>). Both of them radiographically confirmed the successful creation of congenital spinal deformity mice, but did not follow those individuals up chronologically. Especially when discussing about the spinal deformity under the influence of the growth, we think it is very important to follow up the same individuals chronologically to observe the real change over time, which are feasible with the animal models for their shorter life cycle. Detailed and repetitive observation of the younger malformed vertebrae with MRI would bring us about further information for the congenital scoliosis from not only osseous but also soft tissue structures, which neither radiographic modalities nor histological analysis could provide. However, we could find neither the report on the chronological change nor MRI of animal congenital spinal deformities. In a previous report, we analyzed anatomical structure of the temporomandibular joint of the mouse by MR microimaging with voxel resolution of 65  $\mu\text{m}$ , which was proved to be comparable to hematoxylin-eosin staining under light microscopy<sup>12</sup>). With this microscopic ability of our MR microimaging, we thought chronological detailed follow-up of the living mice would become feasible.

The purpose of this study is to set up high-resolu-

tion magnetic resonance imaging capable of observing chronologically on a congenital scoliosis mouse model *in vivo* using magnetic resonance microscopy.

## MATERIALS AND METHODS

This project was approved by the Animal Research Councils of our university by the judgement reference number of 988. In reference to the report by Lordet et al., DBA-1J mice were selected as our model animal<sup>11)</sup>. A male and two female DBA/1J mice were obtained from Charles River Laboratories Japan, Inc. (Tsukuba, Japan), and bred in house by brother-sister inbreeding. Mice were mated and the females found with vaginal plug in the next morning were assumed to be pregnant, and the morning was designated as Day 0.5. Among these females, those with continuous significant increase in their body weight were considered to be with fetuses successfully, and were exposed to Carbon Monoxide (CO) on the Day 9.5. These mice were placed in air-sealed chamber with sufficient water and food, to which the gas cylinder containing compressed air with 600 ppm of CO (TOKAI Corporation, Shizuoka, Japan) were connected. Air with CO were introduced into the chamber at atmospheric pressure under the monitoring of CO and O<sub>2</sub> concentration in the chamber. The gas flow was stopped when CO in the chamber reached above 550 ppm. CO and O<sub>2</sub> concentration in the chamber were kept between 550–600 ppm and above 20% respectively for more than 6 hours, under the occasional check and supply of mixed gas.

The new-born mice were screened for the spinal anomaly with soft x-ray imaging (CMB-2, SOFTEX Co., Ltd., Japan) about 3.5 weeks after birth. The mice with spinal anomaly were followed up with soft x-ray images at intervals of a few weeks. For the soft x-ray imaging the mice were anesthetized with 2% isoflurane and kept supine on a sponge positioner during the x-ray shot.

The mice with spinal anomaly were also followed up with MRI. MR images were obtained by a 7 tesla (T) microimaging system (AVANCE III, Bruker BioSpin, Ettlingen, Germany) with <sup>1</sup>H radiofrequency (RF) surface coil (16 mm in diameter, for 7Tesla, 300 MHz, Doty Scientific Inc, SC, USA). The mouse was anesthetized with 1.5–3% of sevoflurane in mixed gas

of N<sub>2</sub>O and O<sub>2</sub> given through a face mask. In the plexiglass cradle (MRTechnology, Tsukuba, Japan) to which the mouse was fixed with adhesive tape, its heart rate, respiratory rate, body temperature, and blood oxygen saturation (SpO<sub>2</sub>) were continuously monitored. Warm water was perfused in a tubular circuit attached on the belly of the mouse in order to keep the body temperature. Sevoflurane was adjusted to keep the respiratory rate around 30/min so that the respiratory motion artifact from the chest wall could be minimized. Typical parameters used for the three-dimensional T<sub>1</sub>-weighted gradient-echo imaging (3D-T<sub>1w</sub>) by Fast Low Angle Shot (FLASH) were as follows: 19.2×19.2×9.6 mm field of view (FOV), 192×192×96 data matrix, 50 ms repetition time (TR), 3.75 ms echo-time (TE), a flip angle of 22.5°, 1 acquisition, and a total image acquisition time was 15 min 21 s. Images were Fourier transformed with a data matrix 384×384×192 after zero filling of data, and the final voxel resolution was 50×50×50 μm. Three-dimensional T<sub>2</sub>-weighted rapid acquisition with relaxation enhancement (RARE) imaging (3D-T<sub>2w</sub>) was also conducted with the same voxel resolution with a combination of TR/TE/RARE-factor = 1000 ms/50 ms/16, 1 acquisition, and a total image acquisition time was 19 min 12 s. Sinc-shaped pulses was used for excitation and refocusing. The RF power was adjusted using a coronal slice in the depth of the spine with 1 mm thickness. High-resolution images with a voxel size of 50×50×50 μm for PFA fixed spine were measured by a bird cage RF coil (25-mm in diameter) (Bruker BioSpin, Ettlingen, Germany). Parameters for 3D-T<sub>1w</sub> MRI were a combination of TR/TE/flip angle = 50 ms/5.65 ms/22.5°, and a total image acquisition time of 11 h. 3D-T<sub>2w</sub> RARE MR images were obtained with a combination of TR/TE/RARE-factor = 750 ms/50 ms/16, and a total image acquisition time of 5 h. After zero filling of data, and the final voxel resolution was 25×25×25 μm.

Each mouse was scanned alive for three times at intervals. After the last take of serial alive MRI, anesthesia was deepened and mice were euthanized, and another scan was obtained for the dead body in the same posture as its final living scan. After this session, the spine specimens were harvested and fixed in the formalin, and were scanned by soft x-ray and MRI.

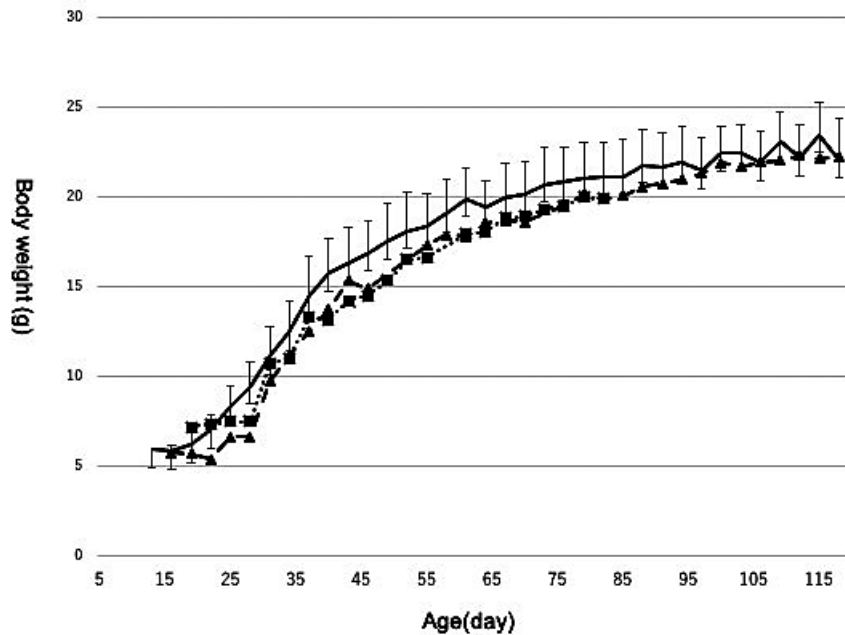


**Fig. 1** Body weight growth of male DBA-1J mice  
 — : Average weight (g) of male mice with 1 Standard Deviation (SD).  
 - -■- - : body weight of Mouse 1, - -▲- - : body weight of Mouse 2.

## RESULTS

Six female mice (3 daughters of the first generation, and 3 daughters of one of these three by brother-sister inbreeding) were assumed to be pregnant and exposed to CO. Among them three delivered ten baby mice in total, and eight of these ten thrived. All of these mice showed no abnormality in appearance, gait, and body weight growth. And by the screening with soft X-ray, two of them were found to have vertebral anomalies; Mouse 1 and Mouse 2. All the mice completed the CO exposure and imaging sessions without any trouble including debility or weight loss. The growth of the body weight of Mouse 1 and 2 are shown in comparison with the average of the other male mice (Fig. 1).

### Mouse 1

Soft X-ray images (Fig. 2)

There are six vertebrae at the lumbar region between the most caudal vertebra with rib and the sacrum. Irregular alignment is seen at thoracolumbar and upper lumbar spine, and rib anomalies are seen at the low thoracic level. In the global coronal view its spinal curvature did not progress all through the

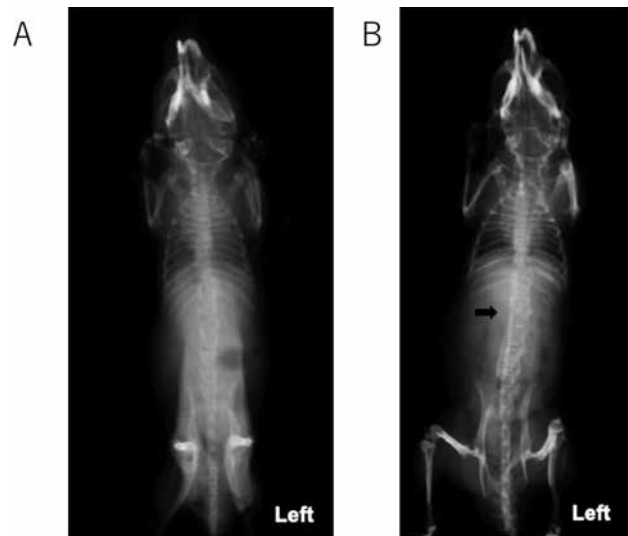


**Fig. 2** Antero-posterior view of the Soft X-ray of Mouse 1  
 Antero-posterior view of the Soft X-ray of Mouse 1. **A)** 5.5 weeks after birth **B)** 27 weeks after birth. At the lower thoracic level, there are rib anomalies. Between the two lowest ribs on the left of the mouse, there is a hemivertebra. Upper lumbar spine the intervertebral disc spaces are not seen (arrow). The local and global alignment of the spine has not largely changed between these two X-ray images.

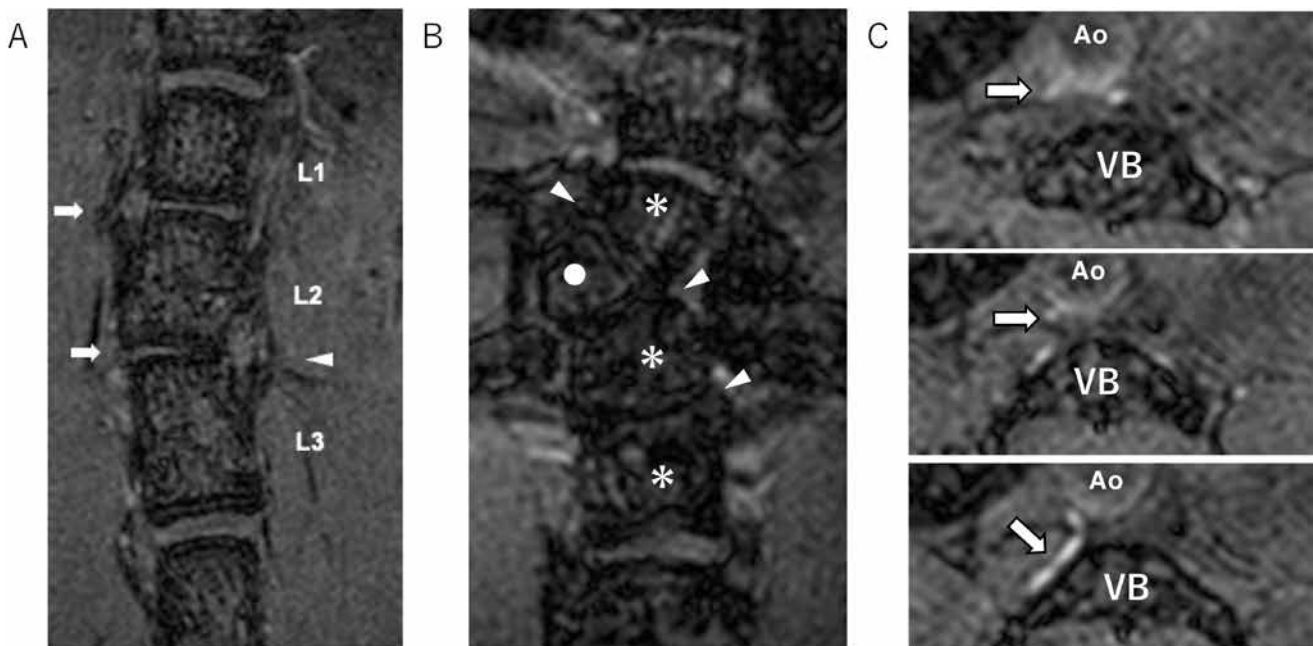


**Fig. 3** MR image of the Mouse 1 (FLASH)

MR image of the Mouse 1 of Fast Low Angle Shot (FLASH). (A) Coronal views of the upper lumbar spine, and (B) the thoracolumbar spine. (C) Axial view of the lumbar spine.

(A) Two of the disc spaces are thinner than others (arrow), and osseous continuation is connecting two vertebrae (arrow head).

(B) There is an unsegmented hemivertebra (●). No disc are seen (arrow head) and four of the (hemi) vertebrae (●, \*) are composing a block vertebra.

(C) Segmental artery (arrow) is branching out of aorta, seen as high intensity line. This is due to the inflow effect on short TR and short TE setting under the surface coil, and fast blood flow in the shallow area is intensified. Ao : aorta, VB : vertebral body

growth. At the bottom of the second lowest rib, spine has minor local curve with small hemivertebra on the convex side. The upper lumbar spine has very small or no intervertebral space compared to the lower lumbar spine. X-ray image of the spine specimen can clearly show the hemivertebra at the thoracolumbar spine.

MRI (Fig. 3)

Mouse 1 was scanned alive with MRI on the 2<sup>nd</sup>, 6<sup>th</sup>, 7<sup>th</sup> months after birth, followed by postmortem and specimen scans. It had an unsegmented hemivertebra at lower thoracic spine with rib anomalies. No disc space could be seen at the cranial and caudal end of the hemivertebra, and the caudal end of the lower adjacent vertebra. The upper lumbar spine (named here as L1, L2, L3) has linear high intensity area at the location where intervertebral spaces are expected, which are much thinner compared to the intervertebral space between T12-L1 or L3-L4. This can be

rudimentary discs or just cartilaginous layer. At the both end of this high intensity, osseous continuation can be seen bridging the adjacent vertebrae, and 3 vertebrae are not segmented. One side of the L2-L3 intervertebral space and the pedicle and lamina of the same side was not segmented. Arteries such as segmental arteries and intercostal arteries are seen as high intensity lines. These local findings and spinal alignment around vertebral anomalies did not change among all scans.

#### Mouse 2

Soft X-ray images (Fig. 4)

There are six lumbar vertebrae. Mouse 2 has apparent scoliosis at the thoracolumbar spine and irregular ribs. At the apex of the curve, neighboring two vertebrae are wedge-shaped, and no intervertebral space can be seen in between. This local scoliosis is compensated in the adjacent part of the spine, and



**Fig. 4** Soft X-ray of Mouse 2  
Soft X-ray of Mouse 2, 12 weeks after birth. There is a curve at the thoracolumbar junction due to asymmetric vertebrae (arrow head), but global coronal balance is well maintained. Abnormal ribs are seen at the deformity level (arrow).

the global coronal alignment is well balanced with their head on the perpendicular bisectors of the pelvis. This local scoliosis and well-balanced global coronal alignment is maintained all through the follow-up.

MRI (Fig. 5)

Mouse 2 was scanned alive with MRI on the 1.5<sup>th</sup>, 2<sup>nd</sup>, 3<sup>rd</sup> months after birth. It had two succeeding wedge vertebrae at the thoracolumbar spine, causing steep local scoliosis and kyphosis. No disc space could be seen between these wedge vertebrae and the cranially adjacent vertebra. On the concave side a conjoined large rib head was connected to these two wedge vertebrae, and on the convex side the cranial wedge vertebra had abnormal rib which had one head with two bodies. Morphologically no apparent change in terms of the spinal deformity was found during this observation period.

## DISCUSSION

Congenital spinal deformities in human, especially in some cases which progress aggressively and can develop thoracic insufficiency syndrome if untreated, need appropriate intervention<sup>2,13</sup>. The proper selection of the patients and the timing of the surgical intervention is the key, and the information to predict the prognosis of these deformities are currently mainly based on the clinical studies of the osseous mor-

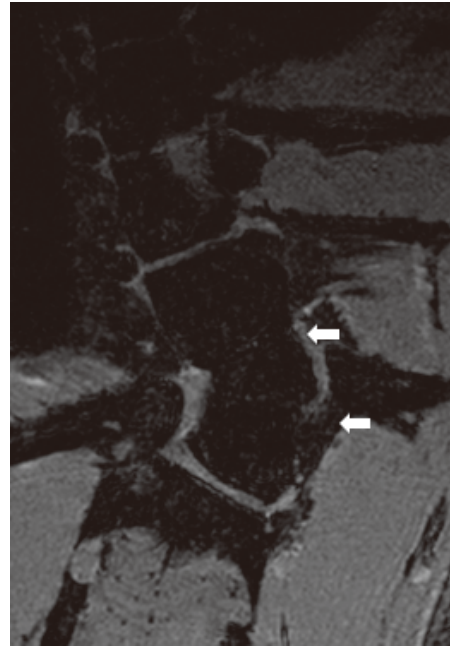


**Fig. 5** MR Image of Mouse 2 (FLASH)  
MR Image of Mouse 2, 12 weeks after birth (coronal view). At the thoracolumbar junction there is a block consisted of three unsegmented vertebrae, two of which are wedge-shaped. No intervertebral space in between (arrows).

phologies by the X-ray or CT scan images. However, modalities using radiation, especially CT scan which requires higher dose of X-ray for osseous structures, are highly concerning for the young growing children. Although the resolution of MRI for bone tissue is not as good as that of CT scans, the ability of MRI to depict the small structures such as intervertebral disc, cartilaginous endplate, or neural tissue precisely without radiation exposure is an indispensable advantage. Additionally, if more information is available from the cartilage or growth plate, which MRI may be able to provide, our prediction can be more accurate and will help us make better strategies for these patients.

DBA/1J mouse reaches reproductive age at 8th weeks after birth, and normal life span is 433 days in males and 750 days in females<sup>14</sup>. Body weight grows rapidly until around 10th week and creeps up thereafter (Fig. 1). Hence, our observation period, which ranges from 3.5 weeks old to 7 months old, corresponds to the period from preadolescence to adult in humans, and should sufficiently cover their growth period. The incidence of our spinal anomalies was

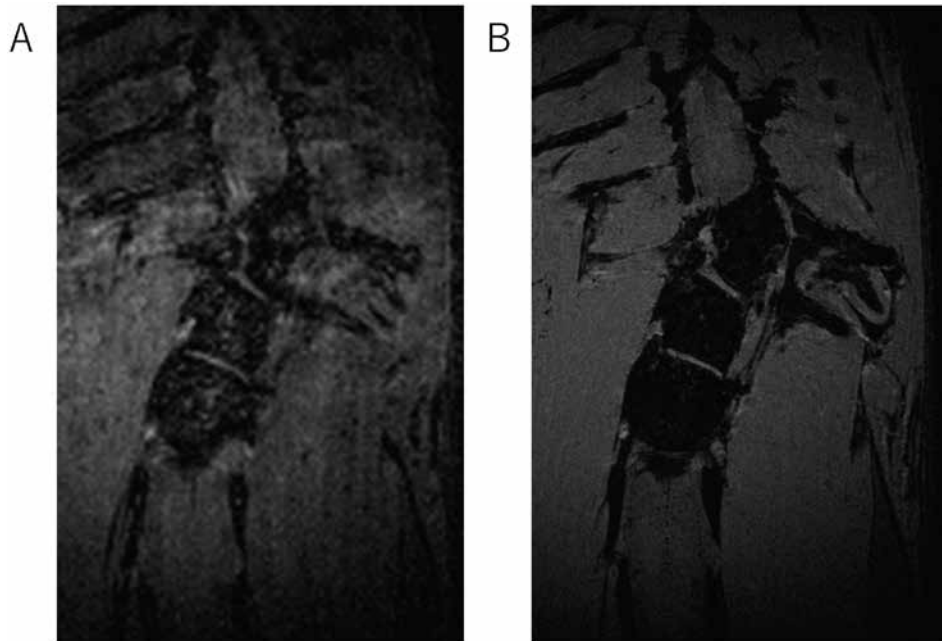


**Fig. 6** MR images of alive and dead mouse (Mouse 2)

MR images of alive and dead mouse, 12 weeks after birth (Mouse 2). **A)** Coronal view of the thoracolumbar spine of alive mouse. **B)** Similar area of the dead mouse. Contour is apparently clear in the image of the dead mouse.

apparently lower than the literature which reported as high as 77%. The lower incidence could be attributable to two reasons ; slightly lower CO concentration and shorter exposure time, and removal of the mice with anomaly. Loder exposed the mice to 600ppm CO for 7 hours. But we kept the CO concentration between 550 and 600ppm, and exposure time was 7 hours including inflation and deflation time which took about 30 minutes. Loder harvested the neonates at the parturition, but we contacted to the mice about 10 days after birth. At least 2 babies disappeared in this period likely due to the removal by the mothers. Eight babies to 3 mothers are much less than the number usually expected, where their litter size are reported as 4.4<sup>14)</sup>, and rodents are known to cannibalize their offspring occasionally, and it has been reported that the newborn with malformations were more frequently cannibalized compared to the normal offspring<sup>15)</sup>.

We could complete five MR scan sessions for both of the deformity model mice. We reconstructed these MR images not in curved but in flat plane so that the description of the morphology at the steep deformity was difficult, and X-ray images were easier to get the

picture of the global alignment. But MRI showed us more detailed information of the small local structures. The small osseous continuation of the block vertebrae and lamina, the absence of the disc space between the wedge vertebrae, the malformation of the base of the ribs could be identified with certainty only with the MRI and could not be detected with soft X-ray images. MRI scan for the thoracic spine were affected by the respiratory motion especially when depicting these fine structures. Because of the anatomical proximity to the thoracic cage, MRI of the thoracolumbar spine of Mouse 1 and Mouse 2 is blurrier compared to that of the lumbar spine of Mouse 1. In order to minimize this effect, we maintained the respiratory rate of the mice around 30/min by adjusting the anesthesia gas. It could be as low as 15/min, but in this lower range the mice respiration become irregular and unstable and would raise the risk of the respiratory arrest, which have to be avoided for the chronological repetitive scan along with the growth of the mice. However, it still provides us with detailed and fine description of these small vertebrae and disc materials compared to the x-ray images.

In each mouse the last two MR images were taken

just before and after the euthanasia without changing the position in the cradle. Several differences could be found by comparing these dead and alive images. The motion artifact was apparent in the alive image especially in the chest. The difference was apparent in the spine images (Fig. 6). Contour of the osseous structures was sharp and clear in the dead image. The diaphragms, and the lung were blurry in the alive image, comparing to the dead image where the vessels in the lung could be clearly seen. The other point is that the fast blood flow, for example the segmental arteries or intercostal arteries, could be seen in the alive image (Fig. 3c).

In terms of the chronological changes in the MRI, we could not find apparent trend morphologically. All of three areas of the malformed vertebrae looked like a block over time. We expected any changes of the morphology or the signal in the adjacent discs or end-plate cartilage which are often seen in humans due to the non-physiological mechanical stress from the malalignment, but in vain. In the vertebrae, spotty dark intensity area became denser and wider, and whole vertebrae appeared darker over time. This likely represents the development of the trabecular bone. On the caudal and cranial edge of the vertebra facing to the disc space there is a layer with darker intensity than vertebra. This is possibly the growth plates which can stay as late as 1 year old in mice<sup>16</sup>. However, this layer can be also seen in the malformed vertebrae, albeit thinner than normal (Fig. 7). If this layer represents active growth plate, scoliosis progression can be expected, which we did not see in our cases. No literature could be found regarding the appearance and changes of the growth plate of mice on MRI, and direct comparison with histology is necessary to confirm.

The weak point of this study is that we could only observe three anomalies in two cases. We could not find the specific characteristics of the progressing spinal curve because of the lack of such cases, and this should be undertaken. The larger number of the cases should be collected for the further findings within the limit of the bioethics. The other point is we performed only the morphological observation of these anomalies. Histopathological observation along with the comparison of them to MRI, for example, would bring us fur-

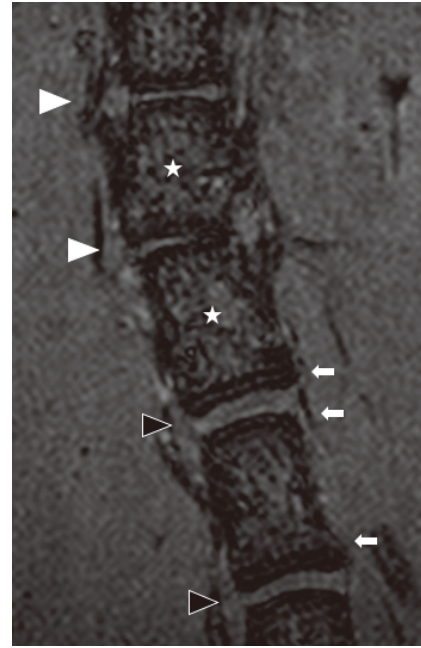


**Fig. 7** MR image of the lumbar block vertebra of Mouse 1 (FLASH)

MR image of the lumbar block vertebra of Mouse 1 (FLASH). Coronal image of the lumbar block vertebra (★) at the age of 1 month. There are double lines at the end plate (arrows) facing to the normal intervertebral discs (black arrow heads), but these lines are indistinguishable at the level facing to insufficient disc space (white arrow heads). These double lines can be the growth plate at the normal structure.

ther information to understand the characteristics of these deformities. Following study should be warranted on this topic.

## CONCLUSION

Congenital scoliosis model mice were produced by maternal carbon monoxide exposure during pregnancy and could be chronologically observed over their growth with soft X-ray and 7T MRI. All of the vertebral anomalies and spinal deformities could be detected in live with the voxel resolution of  $50 \times 50 \times 50 \mu\text{m}$  comparable to low-powered light microscopy. MRI were very powerful to depict the local morphology and distinguish osseous and intervertebral structures of the small mice spine, which soft X-ray image could only show their global curve appearance.

## ACKNOWLEDGEMENT

The authors appreciate Ms. Yoshie Ohashi and Ms. Mika Hayakawa (Dokkyo Medical University School of Medicine) for their contribution in MRI technical assistance.

## DISCLOSURE STATEMENT

This study received financial grant support from Lilly. The authors have no other conflict of interest relating to this work.

## AUTHOR CONTRIBUTION

Conception and design of the study : H.U., T. I., H. M., S. I., H. A., Y. S., H. T.

Acquisition and analysis of data : H.U., T. I., Y. S.,

Drafting the manuscript : H.U., Y. S., H. T.

Others :

## REFERENCES

- 1) Hedequist D, Emans J. : Congenital Scoliosis A review and update. *J Pediatr Orthop* **27** : 106-116, 2007.
- 2) Winter RB, Moe JH, Eilers VE. : Congenital Scoliosis A Study of 234 Patients Treated and Untreated : PART I : NATURAL HISTORY. *J Bone Joint Surg* **50** : 1-15, 1968.
- 3) Karol LA, Johnston C, Mladenov K, et al : Pulmonary Function Following Early Thoracic Fusion in Non-Neuromuscular Scoliosis. *J Bone Joint Surg Am* **90** : 1272-1281, 2008.
- 4) Karol LA : Early Definitive Spinal Fusion in Young Children : What We Have Learned. *Clin Orthop Relat Res* **469** : 1323-1329, 2011.
- 5) Reames DL, Smith JS, Fu KG, et al : Complications in the surgical treatment of 19,360 cases of pediatric scoliosis : a review of the Scoliosis Research Society Morbidity and Mortality database. *Spine* **36** : 1484-1491, 2011.
- 6) McMaster MJ, Ohtsuka K. : The natural history of congenital scoliosis. A study of two hundred and fifty-one patients. *J Bone Joint Surg Am* **64** : 1128-1147, 1982.
- 7) John E, Lonstein, Robert B, Winter, David S Bradford, et al : Moe's Textbook of Scoliosis and Other Spinal Deformities 257-294, 1995.
- 8) Farley FA, Hall J, Goldstein SA. : Characteristics of Congenital Scoliosis in a Mouse Model. *J Pediatr Orthop* **26** : 341-346, 2006.
- 9) Sparrow DB, Chapman G, Smith AJ, et al : A Mechanism for Gene-Environment Interaction in the Etiology of Congenital Scoliosis. *Cell* **149** : 295-306, 2012.
- 10) Farley FA, Loder RT, Nolan BT, et al : Mouse Model for Thoracic Congenital Scoliosis. *J Pediatr Orthop* **21** : 537-540, 2001.
- 11) Loder R, Hernandez M, Lerner AL, et al : The Induction of Congenital Spinal Deformities in Mice by Maternal Carbon Monoxide Exposure. *J Pediatr Orthop* **20** : 662-666, 2000.
- 12) Yamazaki F, Satoh K, Seo Y : Structure and size-selective permeability of the temporomandibular joint of the mouse measured by MR Imaging at 7T. *Magn Reson Med Sci*, **14** : 115-122, 2015
- 13) Campbell Jr RM, Smith MD, Mayes TC, et al : The characteristics of thoracic insufficiency syndrome associated with fused ribs and congenital scoliosis. *J Bone Joint Surg Am* **85** : 399-408, 2003.
- 14) Mouse Genome Informatics. Inbred Strains of Mice : DBA URL ; [http://www.informatics.jax.org/inbred\\_strains/mouse/docs/DBA.shtml](http://www.informatics.jax.org/inbred_strains/mouse/docs/DBA.shtml)[http://www.informatics.jax.org/inbred\\_strains/mouse/docs/DBA.shtml](http://www.informatics.jax.org/inbred_strains/mouse/docs/DBA.shtml).
- 15) Schardein JL, Petrere JA, Hentz DL, et al : Cannibalistic traits observed in rats treated with a teratogen. *Lab Anim* **12** : 81-83, 1978.
- 16) Zhang Y, Lenart BA, Lee JK, et al : Histological features of endplates of the mammalian spine : from mice to men. *Spine* **39** : E312-E317, 2014.